

# We are IntechOpen, the world's leading publisher of Open Access books Built by scientists, for scientists

6,900

Open access books available

186,000

International authors and editors

200M

Downloads

Our authors are among the

154

Countries delivered to

TOP 1%

most cited scientists

12.2%

Contributors from top 500 universities



WEB OF SCIENCE™

Selection of our books indexed in the Book Citation Index  
in Web of Science™ Core Collection (BKCI)

Interested in publishing with us?  
Contact [book.department@intechopen.com](mailto:book.department@intechopen.com)

Numbers displayed above are based on latest data collected.  
For more information visit [www.intechopen.com](http://www.intechopen.com)



---

# **Intelligent System for Controlling a Three-Phase Active Filter**

---

Raluca Rob, Gelu Ovidiu Tirian and Caius Panoiu

Additional information is available at the end of the chapter

<http://dx.doi.org/10.5772/63640>

---

## **Abstract**

This chapter describes the base algorithm and the implementation of a three-phase active filter controlled by a LabVIEW software application. This intelligent system was designed for power quality improvement in functioning of an electrothermal installation with electromagnetic induction. The active filtering device is composed by pulse width modulation (PWM) converter, which processes the power and the controller that is responsible for signal processing. The PWM converter accomplishes the current compensation from the power distribution. The filter controller processes the signal for a real-time determination of the references for instantaneous compensating current. These currents are continuously supplying the PWM converter. The LabVIEW application is also responsible for the electric parameter's computing. The application uses a data acquisition board connected to a computer and an active filter realized with insulated gate bipolar transistors (IGBTs). This work also contains real measurement sets and parameter variation obtained by using the presented soft-controlled device.

**Keywords:** active filtering, current harmonic compensation, frequency modulation, electrothermal installation, electrical parameters, Labview, data acquisition

---

## **1. Introduction**

The nonlinear elements contained by electrothermal installation lead to three main negative effects, which are reflected in the power quality: circulation of reactive power, appearance of harmonic currents and unbalance of the power supply system.

The problems that appear in power quality are due to the functioning of static electronic converters, power electronic devices, arc furnaces or fluorescent lamps. The frequency

converters, which come in the electric scheme of the electrothermal installation, develop unfavourable effects into the power system: distortion regime generated by the voltage or current waveform, additional heating developed by the high value of the effective currents, or cable insulation damage. These problems can lead to malfunctioning of other electric devices, which are supplied from the same power distribution and also a quality diminution in electric power delivering [1].

## 2. Description of the intelligent system for controlling a three-phase active filter

### 2.1. Electrothermal installation based on electromagnetic induction studied as a generator of distorting regime into the power distribution

#### 2.1.1. The electric scheme of the electrothermal installation

The electric scheme of the electrothermal device has a diode bridge rectifier and an inverter source. Therefore, it represents a current harmonic source. The current waveforms are deeply distorted from the sinusoidal shape, the harmonic current amplitudes are more influenced by the impedance of the power system, and the rectified voltage is less dependent on it.

### 2.2. Technical characteristics of the electrothermal installation

The hardening of electrothermal installation presented in **Figure 1** is composed of a converter CTC100K15 and two inductors for hardening the materials. CTC100K15 has the following electric characteristics: supplying voltage  $3 \times 400$  V, 50 Hz, rated current 27 A, control voltage 24 Vdc, consumed power at high frequency 15 kW, voltage at medium frequency 500 Vac.

-Power supply system. The electrothermal installation is supplied from the three-phase power distribution on 0.4 kV, through a general distribution board.

-Solid-state relay. The on/off switching of the installation is made with three static contactors WG480-D50Z (Solid-state relay-SSR).

-Diode bridge rectifier. In the electric scheme, two diode bridge rectifiers KBPC 3508 are introduced with the following electric characteristics: maximum recurrent peak reverse voltage of 800 V, maximum RMS bridge input voltage of 560 V, maximum forward voltage drop per element of 1.2 V and maximum reverse current at rated DC blocking voltage per element of  $1 \mu\text{A}$ .

-Single-phase inverter. In order to control the frequency in the hardening process, an inverter with four IGBT transistors is used: FF150R12KS4 with the following characteristics: collector-emitter breakdown voltage of 1200 V, collector-emitter saturation voltage of 3.2 V and continuous collector current  $I_{C_{\max}} = 225$  A.

-High-frequency transformers. For supplying the hardening inductors, the electrical scheme contains two high-frequency toroidal transformers—T1: 660/500 V, 40 kVA, 70/100 kHz; T2: 500/500 V, 15 kVA, 70/120 kHz.

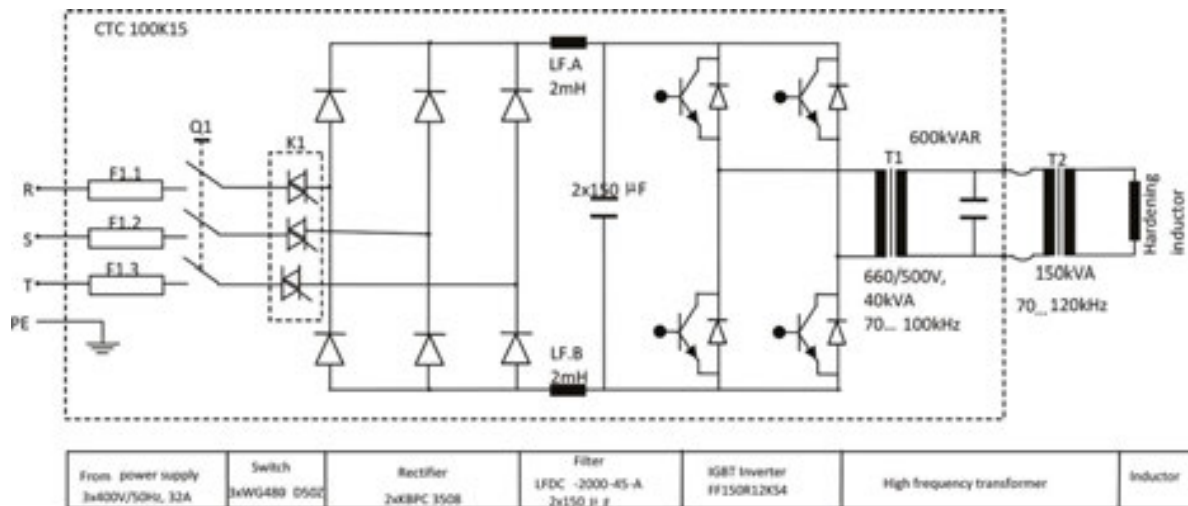


**Figure 1.** The electric scheme of the electrothermal installation.

### 2.2.1. Measurements of the electrical parameters using a data acquisition system

Data acquisition system (**Figure 2**) also follows the acquisition of samples from phase voltages and phase currents at the point of common coupling. In order to accomplish the system for measuring and computing the electrical parameters acquisition, an adapting block and a data acquisition board connected to a computer were used. The connection of data acquisition system to PCC [2] is presented in **Figure 2**. The phase voltages and phase currents were acquired using the adapting block, which was designed in order to accomplish the galvanic isolation between the electrothermal installation and the data acquisition system and also to realize the compatibility of the voltage levels. The data acquisition board has the following main characteristics: 16 analogic inputs with 16-bit resolution and 250 kS/s, two analogic outputs with 16-bit resolution and 740 kS/s, and 24 TTL digital in/out and one digital trigger.

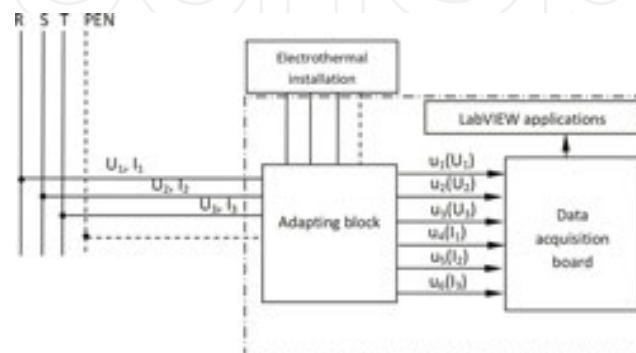


**Figure 2.** Connection to the power distribution of the data acquisition system.

In order to process the acquired data, two soft applications designed in LabVIEW 2011 were used: an acquisition application and a computing application. Using the acquisition application, the voltage and current samples are stored into a file. This file is loaded by the computing application, which is able to compute the most important electrical parameters that characterize the functioning of the electrothermal installation.

The algorithm configures 10 analogical input channels. The maximum sampling rate provided by the acquisition device is 250 kS/s, so, the maximum sampling rate for one channel is 25 kS/s. Equation (1) defines the number of samples on each period:

$$N = f_s \cdot T = 25 \text{ kS/s} \cdot 0.02 \text{ s} = 500 \text{ samples} \quad (1)$$

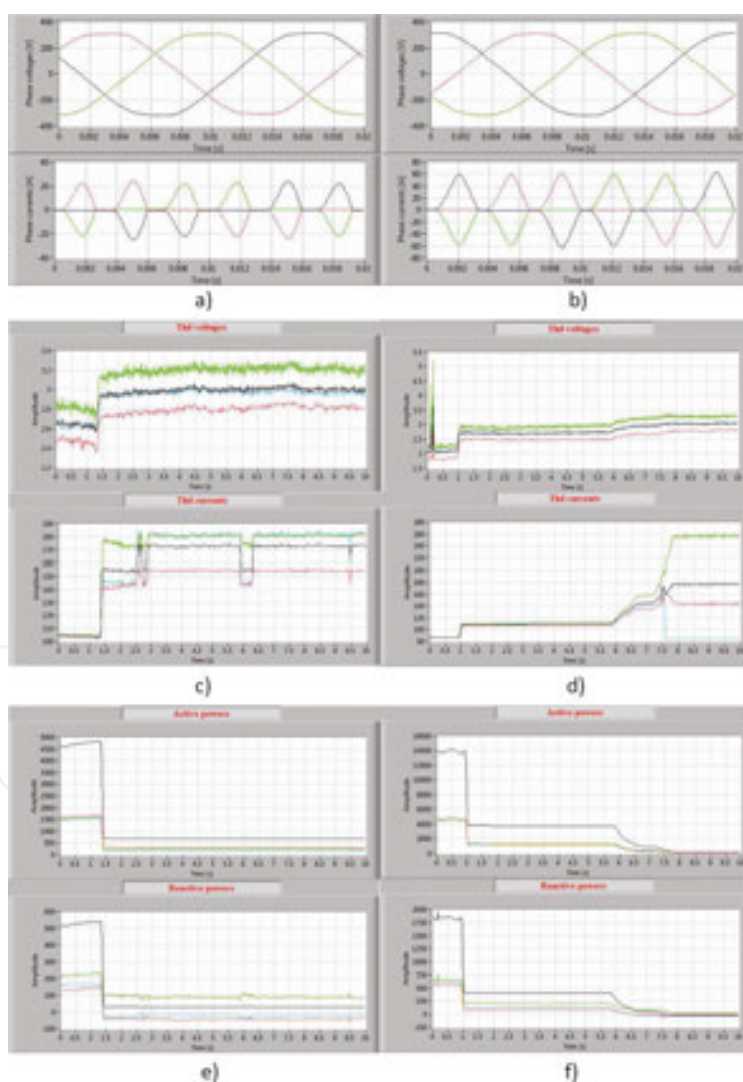


**Figure 3.** The variation of the electrical parameters: (a, b) Phase voltages and currents on 20 ms for 4.5 and 15 kW; (c, d) THD of voltages and currents on 10 s for 4.5 and 15 kW; (e, f) active and reactive powers on 10 s for 4.5 and 15 kW.

The acquisition is developed on a 10-s interval. The number of the acquired samples on each channel is 250,000. Using presented applications, 10 measurement sets were accomplished by increasing with 10% the power of electrothermal installation. In **Figure 3**, the variation on 0.02 and 10 s for phase voltages, phase currents, and also the variation on 10 s of total harmonic distortion (THD) for phase voltages, phase currents and the active and reactive powers are presented when the absorbed power of the power installation is 4.5 and 15 kW. Some observations must be made. In figures that represent the variation form of the currents and voltages, on period of 0.02 s, phase 1 is red, phase 2 is green and phase 3 is blue. For the variations on 10 s, the colour signification is black for all three phases, red for phase 1, green for phase 2 and blue for phase 3.

In **Table 1**, the electrical parameters obtained by accomplishing 10 measurement sets using data acquisition system are synthesized. In **Figure 4**, the variation of the current and voltage harmonic spectrum is presented. **Table 2** presents the harmonic current values.

Absorbed power (kW)	Phase voltages (V)	Phase currents (A)	THD voltages (%)	THD currents (%)
1.5	226.5	3.5	2.95	140
3	227.0	6.0	2.80	120
4.5	226.5	10.0	2.65	105
6	226.6	10.5	2.70	105
7.5	226.5	11.0	2.65	100
9	226.5	13.0	2.50	98
10.5	226.3	15.5	2.40	95
12	227.0	19.0	2.35	92
13.5	227.0	24.0	2.10	90
15	226.5	28.0	2.00	85

**Table 1.** Electrical parameters measured with data acquisition system.

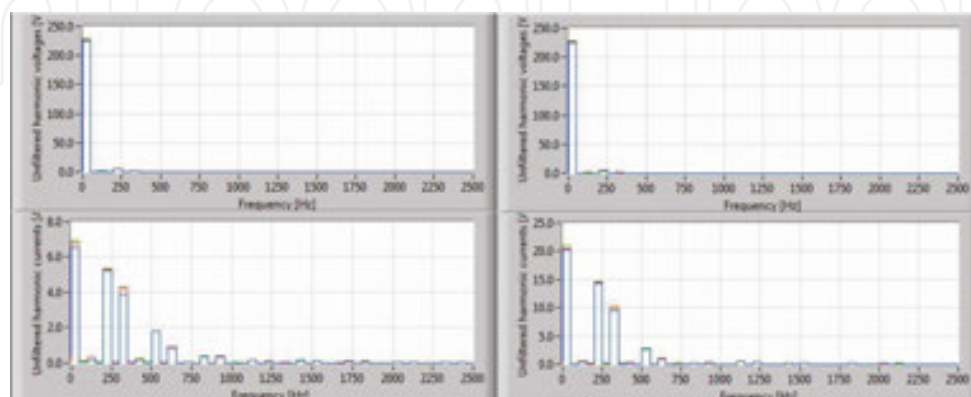


**Figure 4.** The variation of the current and voltage harmonic spectrum: (a) for 4.5 kW; (b) for 15 kW.

Installation power (kW) Rank →	Harmonic currents (A)									
	1	3	5	7	9	11	13	15	17	19
3.0	4.0	–	3.0	2.7	–	1.5	1.0	0.3	0.1	–
4.5	6.7	–	5.0	4.0	–	2.8	1.0	0.1	–	–
6.0	6.0	–	4.3	3.8	–	1.8	1.0	–	–	–
7.5	8.0	–	6.0	4.8	–	2.0	1.5	0.2	–	–
9.0	9.2	–	7.0	5.3	–	2.0	1.5	0.1	–	–
10.5	11.5	–	8.0	6.0	–	2.0	1.5	0.1	–	–
12.0	14.0	–	10.0	7.5	–	2.4	1.8	–	–	–
13.5	17.0	–	12.5	9.5	–	2.4	1.9	–	–	–
15.0	20.0	–	15.0	10.0	–	2.5	2.0	–	–	–

**Table 2.** Current harmonic spectrum.

The data acquisition system presents the advantage of permanent improvement concerning the soft applications that compute the electrical parameters in real time. The application displays the variation on 0.02 and 10 s of the phase voltages, phase currents, THD for phase voltages and phase currents and also the variation of active and reactive powers.

By studying **Figures 3** and **4**, we can conclude that the voltages are balanced and symmetrical and THD for phase voltages are approximately constant and can be neglected. By studying **Figure 3**, we can observe that the variation on 10 s presents three stages. Studying **Table 1**, the values of the phase currents are increasing (3.5/28 A) and the THD for phase currents are decreasing (140/85 A) with the increasing of the absorbed power. Even in this situation, the values of THD for phase currents fall below standard limits. The most important conclusion is that the harmonic currents must be compensated using appropriate devices. **Table 3** synthesizes the values for the electrical parameters.

Electrical parameters	Measurements with data acquisition system	
	4.5 kW (30% P <sub>n</sub> )	15 kW (100% P <sub>n</sub> )
Phase voltage (V)	226.5	226.5
Phase current (A)	10	27
Active power (W)	4700	14,000
Reactive power (VAr)	500	2000
THD voltages (%)	2.65	2
THD currents (%)	105	85

**Table 3.** Measured and computed values for the electrical parameters.



## 2.3. Designing of the harmonic compensation equipment

In order to compensate the harmonic distortion, the electrothermal installation must be equipped with harmonic compensation devices for bringing the parameters into standard limits. Therefore, a power-quality improvement system was designed. For decreasing the total harmonic distortion of the phase currents, the system contains a three-phase passive filtering system accorded on 5th, 7th, 11th and 13th harmonic currents and a shunt active filter, which controls an IGBT module using the software application. The function of monitoring the electrical parameters and controlling the hardware devices is accomplished by a LabVIEW application. As well, this application is able to generate pulses to command the active filter and also to receive the compensating currents [3] by data acquisition board. In **Figure 5**, the block scheme with the connection of the harmonic compensation devices is presented.

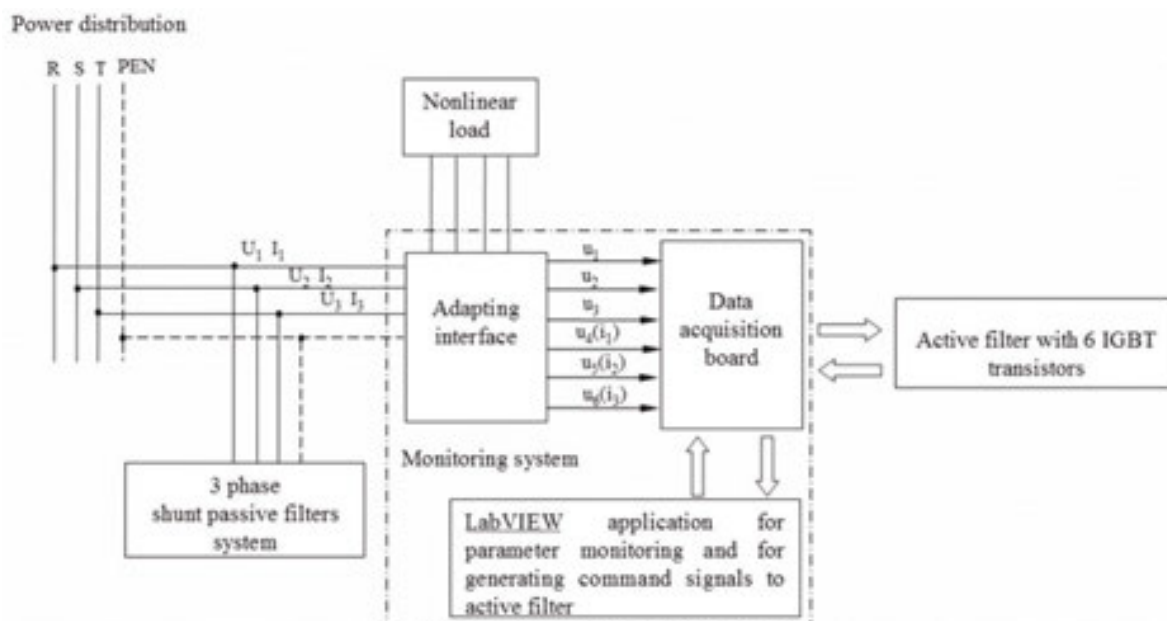


**Figure 5.** The connection of the harmonic compensation equipment.

### 2.3.1. Harmonic compensation using active filters

Shunt active filter determines in real time the compensating current and commands a power converter to synthesize it accurately.

Shunt active filter generally consists of two main blocks: pulse width modulation (PWM) converter for power processing and the active filter controller for signal processing. The PWM converter is responsible for power processing in synthesizing the compensating current that should be drawn from the power system.

The shunt active filter controller works in a closed-loop manner, continuously measuring the distorted current and computing the instantaneous values of the compensating current for the PWM converters [4].



The PWM converter should have high switching frequency in order to accurately reproduce the compensating currents [5].

The present paragraph details the algorithm for designing a three-phase active filter accomplished with IGBT transistors.

The distorted signals of currents and voltages are assumed by algorithm which uses the Fast Fourier Transformer for extracting the phase and the amplitude of the fundamental component.

The signals, which represent the fundamental components for the current and voltages, are calculated in complex form as Eqs. (2) and (3):

$$\underline{I}_{11} = I_{11} \cdot e^{j\theta_{11}}, \underline{I}_{21} = I_{21} \cdot e^{j\theta_{21}}, \underline{I}_{31} = I_{31} \cdot e^{j\theta_{31}} \quad (2)$$

$$\underline{U}_{11} = U_{11} \cdot e^{j\theta_{11}}, \underline{U}_{21} = U_{21} \cdot e^{j\theta_{21}}, \underline{U}_{31} = U_{31} \cdot e^{j\theta_{31}} \quad (3)$$

where  $I_{ik}$  represents the effective value of  $I_{ik}$ ,  $\theta$  is the phase difference,  $i$  is the phase and  $k$  is the current harmonic order.

The notations for the voltages are the same.

The positive sequence components of the voltages and currents are calculated by the algorithm. For generating the variation form of the positive sequence components, the application follows sinusoidal signal generators. The amplitudes of the generated signals are equal to the modules of the current fundamental component.

The residual currents result by subtracting the positive sequence of the fundamental components from distorted currents.

Using the symmetrical component method, the positive and negative components of the fundamental components of the current and voltage can be determined as in the relations:

$$\underline{I}_{11}^+ = \frac{1}{3}(\underline{I}_{11} + a \cdot \underline{I}_{21} + a^2 \cdot \underline{I}_{31}), \underline{U}_{11}^+ = \frac{1}{3}(\underline{U}_{11} + a \cdot \underline{U}_{21} + a^2 \cdot \underline{U}_{31}) \quad (4)$$

$$\underline{I}_{21}^+ = \frac{1}{3}(\underline{I}_{21} + a \cdot \underline{I}_{31} + a^2 \cdot \underline{I}_{11}), \underline{U}_{21}^+ = \frac{1}{3}(\underline{U}_{21} + a \cdot \underline{U}_{31} + a^2 \cdot \underline{U}_{11}) \quad (5)$$

$$\underline{I}_{31}^+ = \frac{1}{3}(\underline{I}_{31} + a \cdot \underline{I}_{11} + a^2 \cdot \underline{I}_{21}), \underline{U}_{31}^+ = \frac{1}{3}(\underline{U}_{31} + a \cdot \underline{U}_{11} + a^2 \cdot \underline{U}_{21}) \quad (6)$$

$$\underline{I}_{11}^- = \frac{1}{3}(\underline{I}_{11} + a \cdot \underline{I}_{21} + a^2 \cdot \underline{I}_{31}), \underline{U}_{11}^- = \frac{1}{3}(\underline{U}_{11} + a \cdot \underline{U}_{21} + a^2 \cdot \underline{U}_{31}) \quad (7)$$

$$\underline{I}_{21}^- = \frac{1}{3}(\underline{I}_{21} + a \cdot \underline{I}_{31} + a^2 \cdot \underline{I}_{11}), \underline{U}_{21}^- = \frac{1}{3}(\underline{U}_{21} + a \cdot \underline{U}_{31} + a^2 \cdot \underline{U}_{11}) \quad (8)$$

$$\underline{I}_{31}^- = \frac{1}{3}(\underline{I}_{31} + a \cdot \underline{I}_{11} + a^2 \cdot \underline{I}_{21}), \underline{U}_{31}^- = \frac{1}{3}(\underline{U}_{31} + a \cdot \underline{U}_{11} + a^2 \cdot \underline{U}_{21}) \quad (9)$$

where  $a$  is the shift operator:

$$a = e^{j \cdot 2\pi/3} \quad (10)$$

The residual currents are obtained by subtracting the positive components of the currents from the distorted signals (input signals)

$$i_{1r}(t) = i_1(t) - i_{11}^+(t), i_{2r}(t) = i_2(t) - i_{21}^+(t), i_{3r}(t) = i_3(t) - i_{31}^+(t) \quad (11)$$

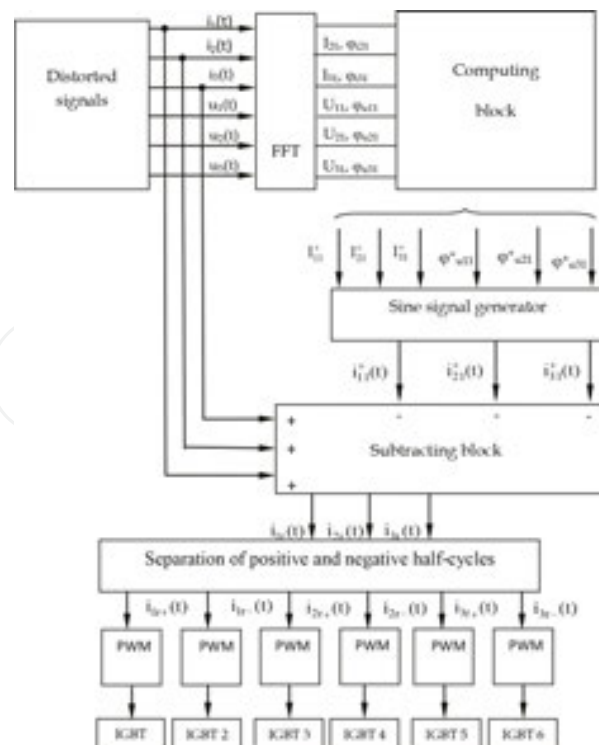


**Figure 6.** Generation of residual currents.

In order to generate PWM pulses proportional to the amplitude of the input signal samples, the algorithm contains six PWM modulators: three for positive and three for negative cycles of the residual currents. The six residual currents,  $i_{1r+}(t)$ ,  $i_{1r-}(t)$ ,  $i_{2r+}(t)$ ,  $i_{2r-}(t)$ ,  $i_{3r+}(t)$ ,  $i_{3r-}(t)$ , are assumed by PWM modulators that generate pulses with the width proportional to the amplitude of the residual signals.

The modulation frequencies  $f_m$  are the following: 2500, 4000, 5000, 10,000 and 12,500 Hz. The block scheme for generating the residual currents is presented in **Figure 6**.

### 2.3.2. Description of the computing application for electrical parameters. Implementation of the active filter algorithm in LabVIEW environment

The LabVIEW computing application has to monitor the electrical parameters and also to control the active filter. This application also receives the compensating currents from the active filter using the data acquisition board [6]. In the following, the computing application is described.

Using the data acquisition board, the computing application can control the active filter system in order to generate the compensation currents.

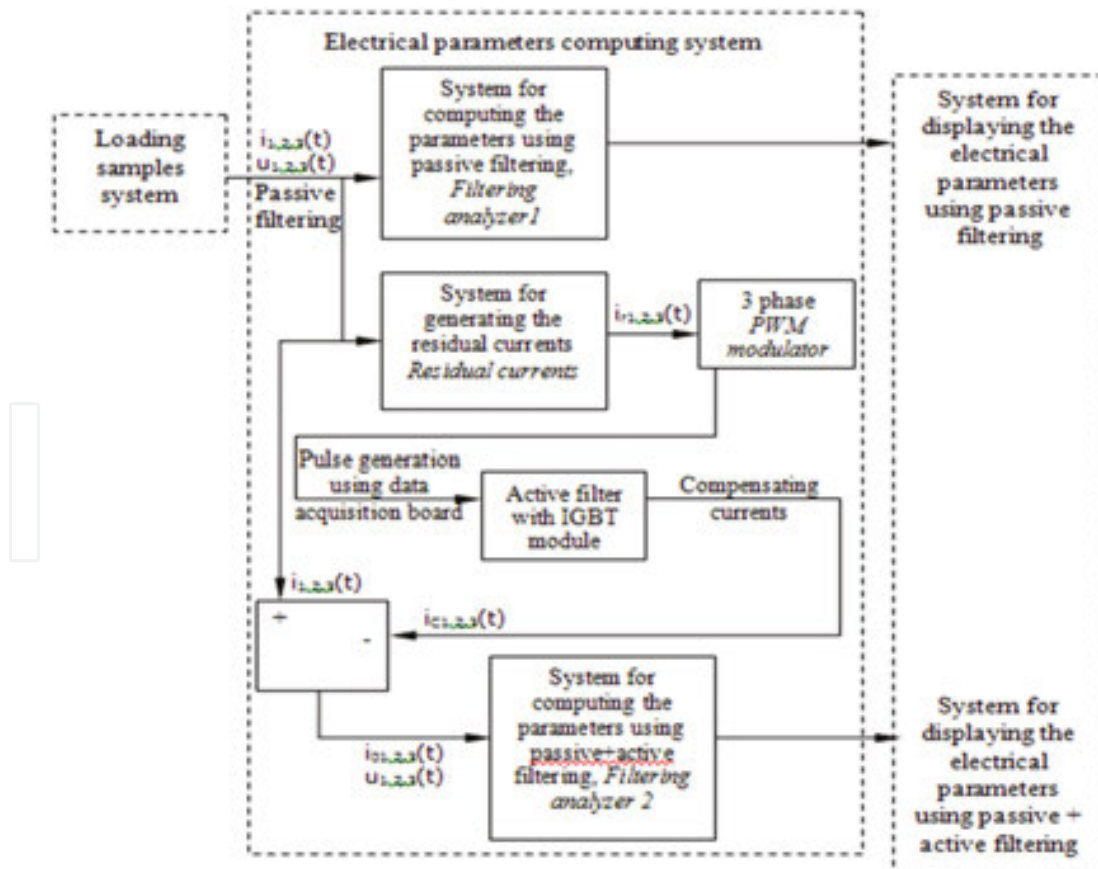


**Figure 7.** Block scheme of the active filtering system.

The control application is accomplished by subroutines which are functioning from the main. The block scheme of the active filtering algorithm is presented in **Figure 7**. The LabVIEW source code is presented in **Figure 8**.

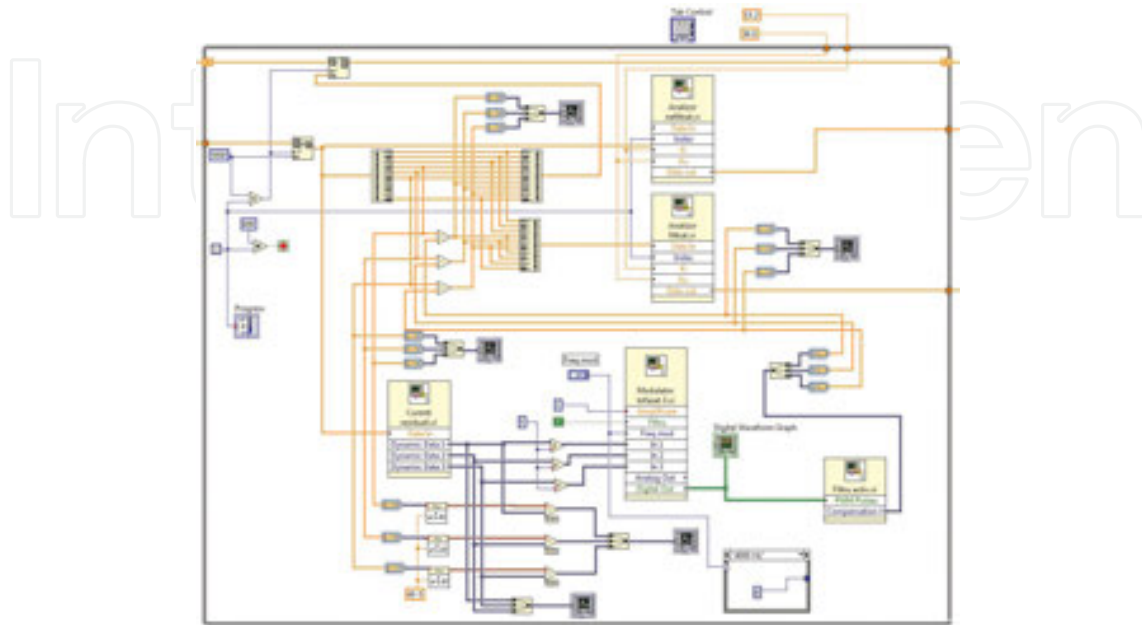


**Figure 8.** LabVIEW source code for computing application.

In the first sequence of the sequential structure which is named *System for loading samples*, the application allows the sample files to be loaded.

These files contain samples from currents and voltages that they have been assumed by the proposed system during the functioning of the electrothermal device when the passive filtering system was connected at the point of common coupling.

#### 2.3.2.1. *System for loading samples*

The algorithm configures 10 analogical input channels.

The maximum sampling rate provided by the acquisition device is 250 kS/s, so, the maximum sampling rate for one channel is 25 kS/s.

The LabVIEW application is structured in such a way that the measuring set can be selected from the front panel. The algorithm generates a vector and its elements are the amplitudes of the assumed samples.

#### 2.3.2.2. *System for electrical parameters computing*

The second sequence of the application contains the computing system, which calculates the electrical parameters using the samples assumed during the functioning of the electrothermal installation equipped with the passive filtering system. The samples of voltage and current

signals are taken from the loading matrix presented in the first sequence. With appropriate functions from LabVIEW library, the algorithm divides the currents from the voltage samples, calculating the effective values of the phase voltages and currents on each period of the power system.

The computing application is structured in subroutines, which will be detailed in the following section.

#### 2.3.2.2.1. Parameter analyser subroutine

The present subroutine computes the electrical parameters that characterize the functioning of the electrothermal installation which are as follows: the effective values for the phase voltage and phase currents, the total values of the voltages and currents, apparent, active, reactive and distorted powers and also the total harmonic distortion of voltages and currents.

In **Figure 9**, the LabVIEW code for the parameter analyser is presented.

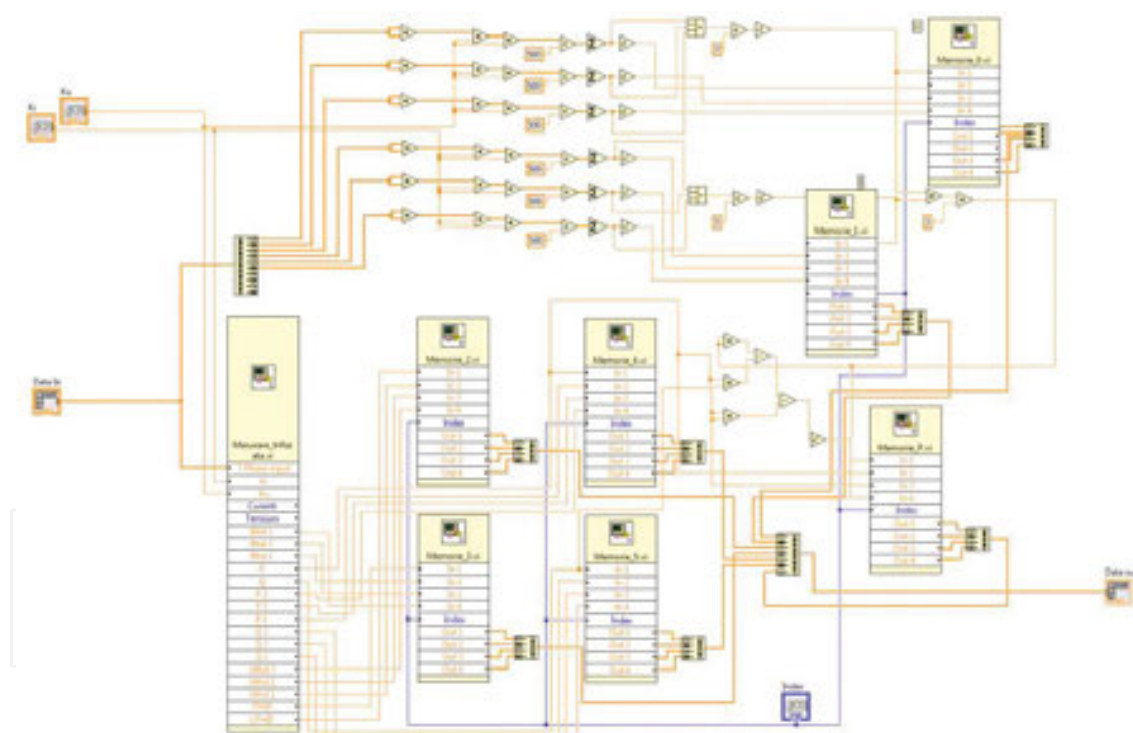


**Figure 9.** LabVIEW source code for parameter analyser subroutine.

#### 2.3.2.2.2. Residual current subroutine

The presented subroutine is based on the algorithm described here and uses another subroutines, *Current phasors* and *Voltage phasors* for computing the positive sequence components of the current and voltage fundamental components.

### 2.3.2.2.3. PWM modulator

The algorithm must generate PWM pulses, which must be proportional with the input signals' sample amplitude; therefore, it includes six PWM modulators: three for negative and three for positive cycles of the residual currents. Mathematical functions from LabVIEW library must separate the cycles. The modulation frequencies for PWM modulators can be selected from the first panel of the application. This property offers a high accuracy level to the output signals.

The PWM modulators are subroutines, which run under the main application. The six residual currents,  $i_{1r+}(t)$ ,  $i_{1r-}(t)$ ,  $i_{2r+}(t)$ ,  $i_{2r-}(t)$ ,  $i_{3r+}(t)$ ,  $i_{3r-}(t)$ , are acquired by PWM modulators, which accomplishes pulses that have proportional width with the amplitude of the residual currents. PWM modulators are presented in **Figure 10**.

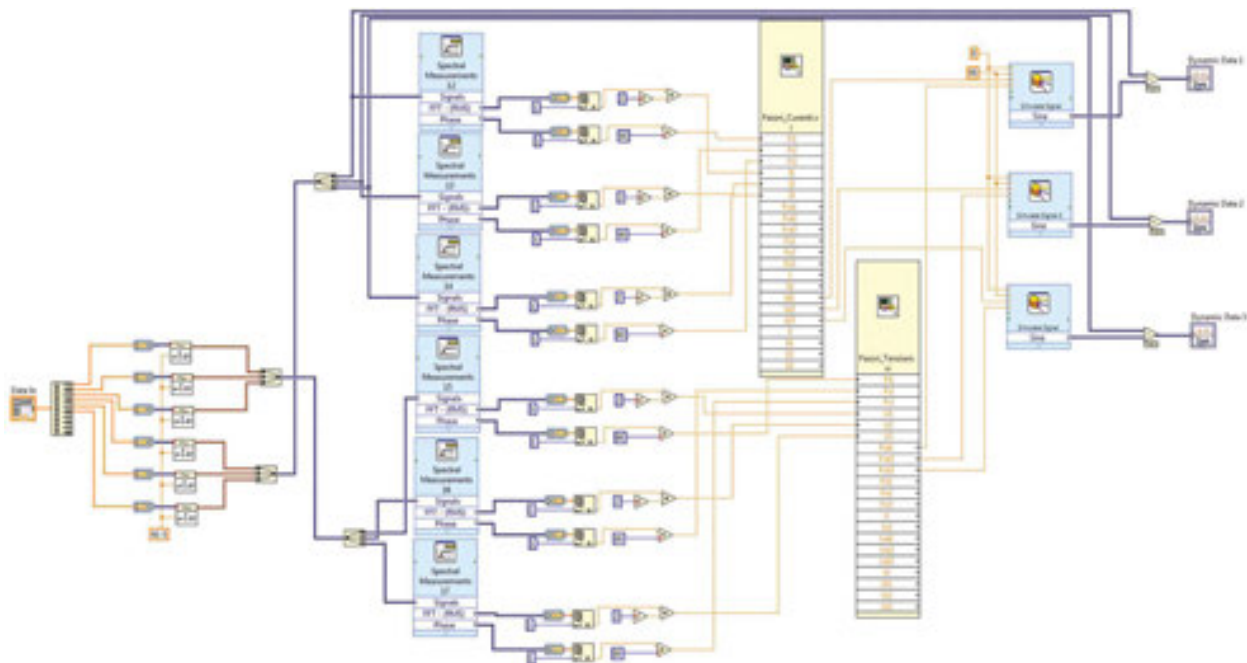


**Figure 10.** LabVIEW source code for residual current subroutine.

The modulation frequencies  $f_m$  are the following: 2500, 4000, 5000, 10,000 and 12,500 Hz and can be chosen from the front panel. Each subroutine generates an array containing a pulse. The sample number for each pulse depends on the maximum internal clock frequency of the acquisition board and also the PWM controller modulation frequencies  $f_m$ , as in Eq. (12):

$$N_{\text{samples}} = f_{\text{clock}} / f_m \quad (12)$$

These number of samples (40, 25, 20, 10 and 8), correlated with frequencies of 2500, 4000, 5000, 10,000 and 12,500 Hz, are used to select the index of the sample, which gives the width of the PWM controller pulse, as in **Figure 11**.



The generated pulses width depends on the residual signal amplitude. In order to determine the generated pulses width, a base of selection of the sample was created, using the residual signal samples. The base of selection represents one one-dimensional (1D) array generated in the following manner: the 500 samples/period of the residual signal are interleaved using the LabVIEW function *Interleave 1D Array*. The algorithm obtains a 1D array of 2000 samples that implies a single residual signal period, sampled four times slower. This array is repeated five times in order to get a new 1D array with 10,000 elements, which was previously mentioned, being the base of selection of the sample.

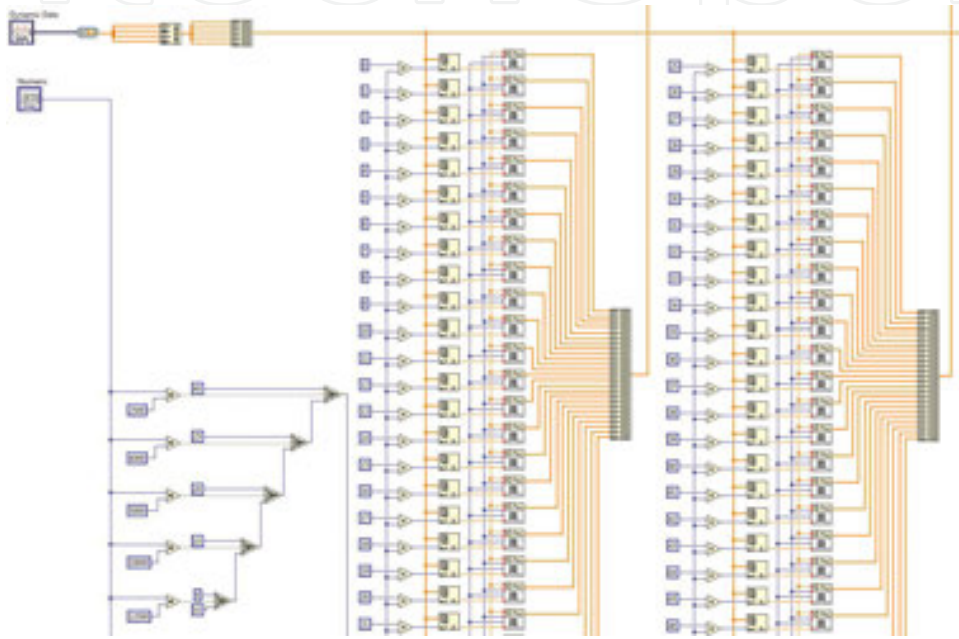


**Figure 11.** PWM modulator for one half-cycle.

The sample selection that determines the pulse width is realized using the function *Index Array* that returns a base of selection element. In the following, the situations that appear by varying the modulation frequency  $f_m$  are related.

If  $f_m = 2500$  Hz, the sample width is taken from index  $n_{2500} = 40 \cdot i$

If  $f_m = 4000$  Hz, the sample width is taken from index  $n_{4000} = 25 \cdot i$

If  $f_m = 5000$  Hz, the sample width is taken from index  $n_{5000} = 20 \cdot i$

If  $f_m = 10,000$  Hz, the sample width is taken from index  $n_{10,000} = 10 \cdot i$

If  $f_m = 12,500$  Hz, the sample width is taken from index  $n_{12,500} = 8 \cdot i$ , where  $i = 0 \dots 249$  represents the order number for the generated pulses.

The number of pulses generated by PWM is 50, 80, 100, 200 and 250 and is correlated with frequencies of 2500, 4000, 5000, 10,000 and 12,500 Hz.

It can be observed that the duration of generated pulses has the lowest value when the modulation frequency has the highest value, but the product of them is a constant equal to 2000.

### 2.3.3. Measurements accomplished during the functioning of the electrothermal installation equipped with harmonic compensation devices

#### 2.3.3.1. Variation of the electrical parameters using passive filtering system

The computing application uses the information from txt files generated when the passive filtering system is connected. In **Figures 12** and **13**, the variation of the electrical parameters on 10 s is presented: phase voltages, phase currents, THD for voltages and currents, and active and reactive powers. The absorbed power of the electrothermal installation is 4.5 and 15 kW and only the passive filtering system is connected. The colour signification for the parameter variation is the following: black for all three phases, red for phase 1, green for phase 2 and blue

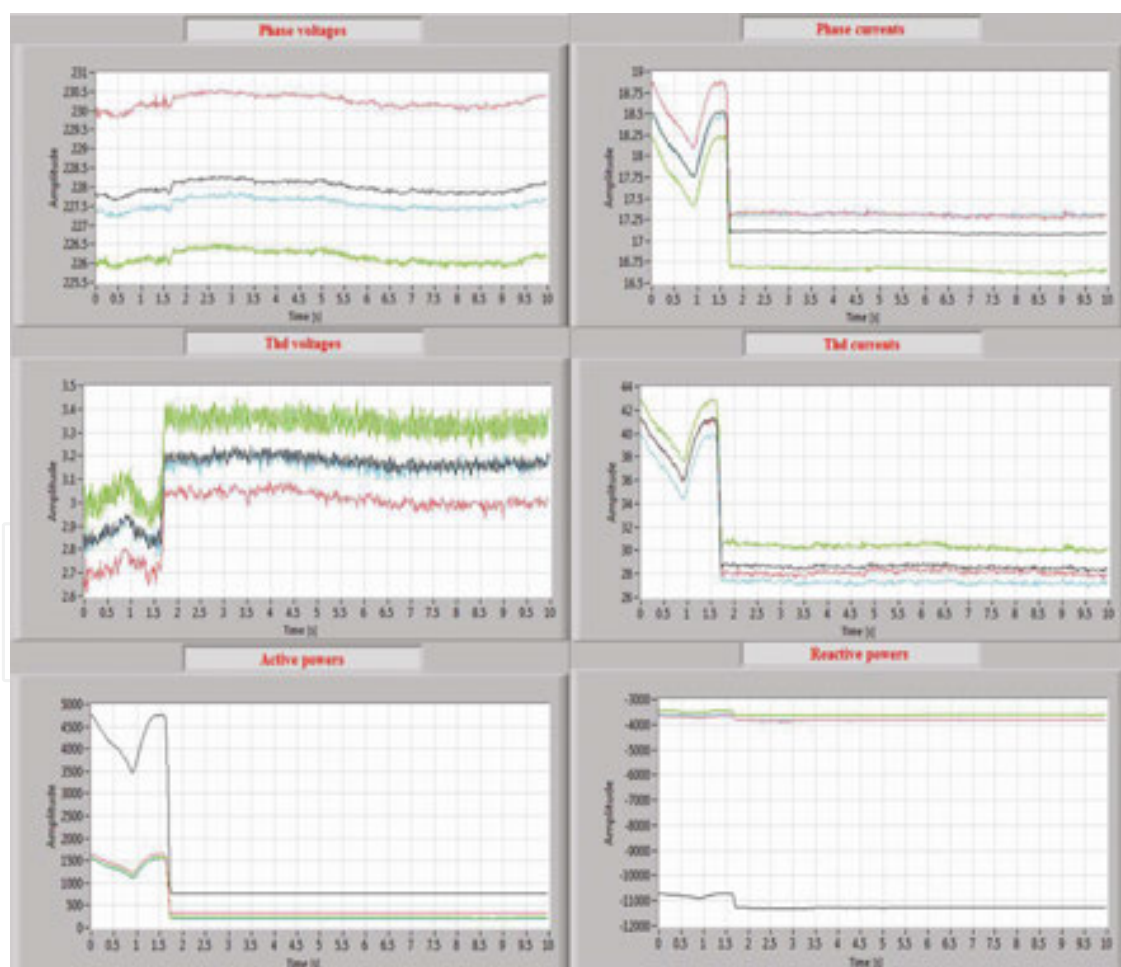


**Figure 12.** Variation of the electrical parameters, passive filtering,  $P = 4.5$  kW.

for phase 3. In **Figure 14**, the variation of the current harmonic spectrum with passive filters is presented.

**Table 4** synthesizes the average values generated by the variation from **Figures 12 and 13**, and **Table 5** synthesizes the values from **Figure 14**.

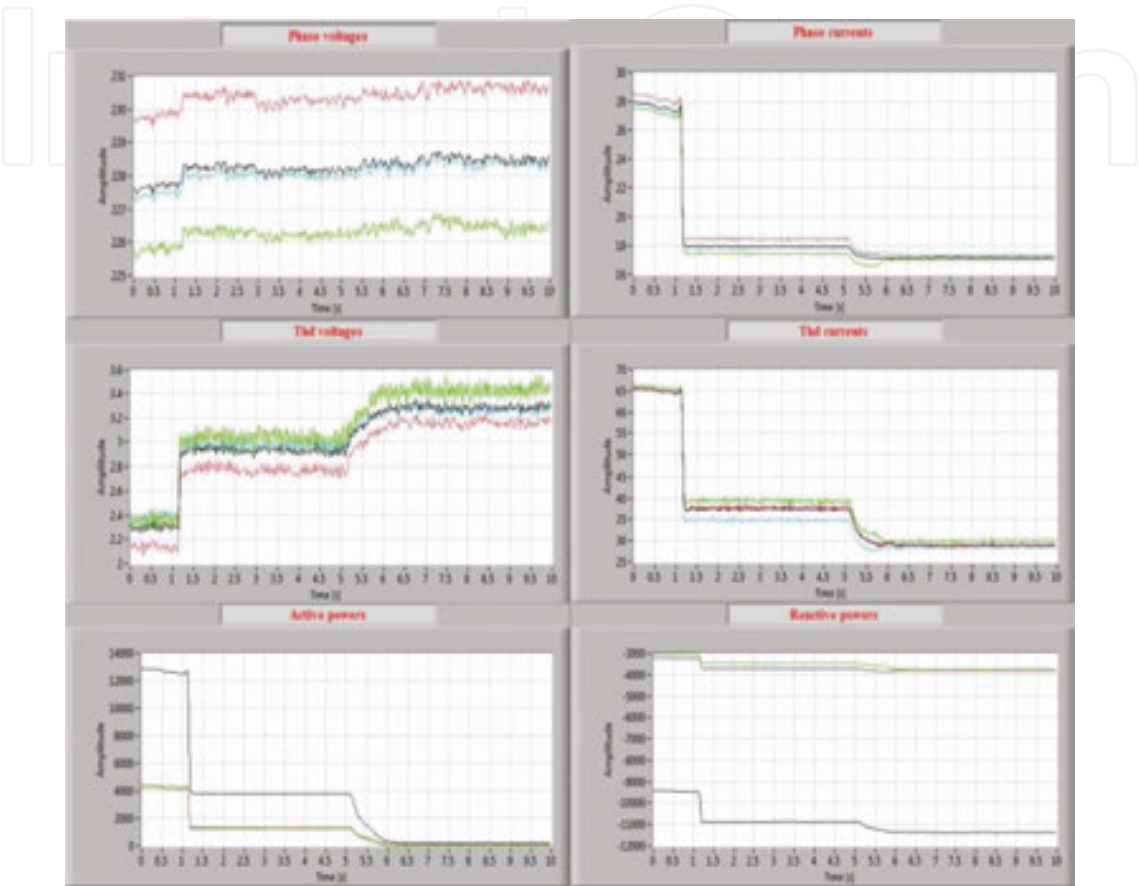


**Figure 13.** Variation of the electrical parameters, passive filtering,  $P = 15 \text{ kW}$ .

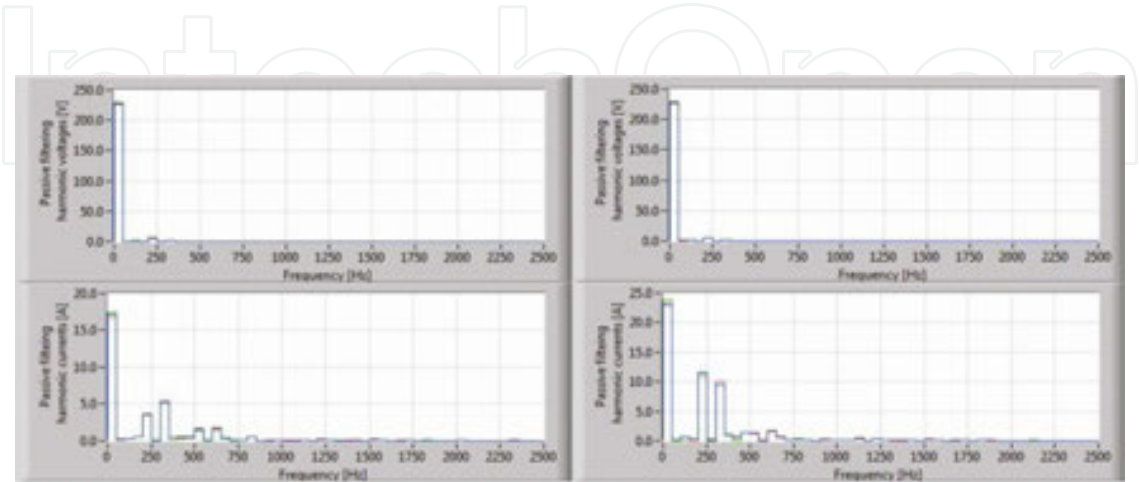


**Figure 14.** Variation of the harmonic current spectrum with passive filtering system (4.5 and 15kW).

Phase voltage (V)	Phase current (A)	Active power (W)	Reactive power (VAr)	Distorted power (VAd)	Apparent power (VA)	THD for voltages (%)	THD for currents (%)
<b>P = 1.5 kW (10% P<sub>n</sub>)</b>							
227.6	17.0	1300	-11,000	3000	11,476	3.15	28.6
<b>P = 3 kW (20% P<sub>n</sub>)</b>							
228.0	17.4	2700	-11,000	3000	11,717	3.00	33.0
<b>P = 4.5 kW (30% P<sub>n</sub>)</b>							
228.0	18.0	4000	-10,800	4800	12,477	2.90	39.0
<b>P = 6 kW (40% P<sub>n</sub>)</b>							
228.0	18.1	4000	-10,800	4800	12,477	2.90	37.0
<b>P = 7.5 kW (50% P<sub>n</sub>)</b>							
228.0	18.7	5000	-10,800	5000	12,909	2.85	42.5
<b>P = 9 kW (60% P<sub>n</sub>)</b>							
228.4	19.3	5800	-10,700	5000	13,158	2.85	45.0
<b>P = 10.5 kW (70% P<sub>n</sub>)</b>							
228.8	19.5	6000	-10,700	6000	13,656	2.80	45.0
<b>P = 12 kW (80% P<sub>n</sub>)</b>							
228.2	22.2	8800	-10,000	7000	15,048	2.65	55.0
<b>P = 13.5 kW (90% P<sub>n</sub>)</b>							
228.0	25.0	11,000	-10,000	8000	16,882	2.50	60.0
<b>P = 15 kW (100% P<sub>n</sub>)</b>							
227.5	28.0	13,000	-9500	10,000	18,954	2.30	65.0

**Table 4.** Electrical parameters obtained with passive filtering system for specified active powers (percent of nominal power).

Active power (Kw) Rank →	Harmonic currents (A)										
	1	3	5	7	9	11	13	15	17	19	21
1.5	16	–	2	4	–	3	2	–	–	–	–
3	16	–	3	4	–	2	2	–	–	–	–
4.5	17	–	4	5	–	2	2	–	–	–	–
6	17	–	3	5	–	2	2	–	–	–	–
7.5	17.5	–	4	6	–	2	2	–	–	–	–
9	18	–	5	6	–	2	3	–	–	–	–
10.5	18	–	5	6	–	2	3	–	–	–	–
12	20	–	7	7.5	–	2	3	–	–	–	–
13.5	21	–	9	8	–	2	2	–	–	–	–
15	23	–	11	10	–	2	3	–	–	–	–

**Table 5.** Average values for the harmonic current spectrum with passive filtering system.

### 2.3.3.2. Variation of the electrical parameters using active filtering system

**Table 6** synthesizes the average values generated by the variation from **Figures 15** and **17**, and **Table 7** works with **Figure 16**.

Phase voltage (V)	Phase current (A)	Active power (W)	Reactive power (VAr)	Distorted power (VAd)	Apparent power (VA)	THD for voltages (%)	THD for currents (%)
<b>P = 1.5 kW (10% Pn)</b>							
228	14.7	9500	-1250	3000	10,041	3.15	16.0
<b>P = 3kW (20% Pn)</b>							
228	15.5	10,500	-800	2000	10,719	3.00	17.5
<b>P = 4.5 kW (30% Pn)</b>							
228	15.8	10,600	-600	2100	10,823	2.90	17.5
<b>P = 6 kW (40% Pn)</b>							
228	15.0	9800	-2000	3000	10,442	2.90	20.0
<b>P = 7.5 kW (50% Pn)</b>							
228	16.0	10,500	-1250	3000	10,991	2.85	20.0
<b>P = 9 kW (60% Pn)</b>							
228.3	16.5	10,800	-1200	2200	11,087	2.85	19.0
<b>P = 10.5 kW (70% Pn)</b>							
228.7	16.5	11,000	-250	2500	11,283	2.80	18.1
<b>P = 12 kW (80% Pn)</b>							
228.3	19.0	12,500	-1200	3000	12,911	2.61	21.0
<b>P = 13.5 kW (90% Pn)</b>							
228	21.5	14,000	-80	2300	14,188	2.50	17.0
<b>P = 15 kW (100% Pn)</b>							
227.8	23.0	15,000	-100	2500	15,207	2.30	17.0

**Table 6.** Electrical parameters obtained with passive and active filtering system for specified active powers (percent of nominal power).

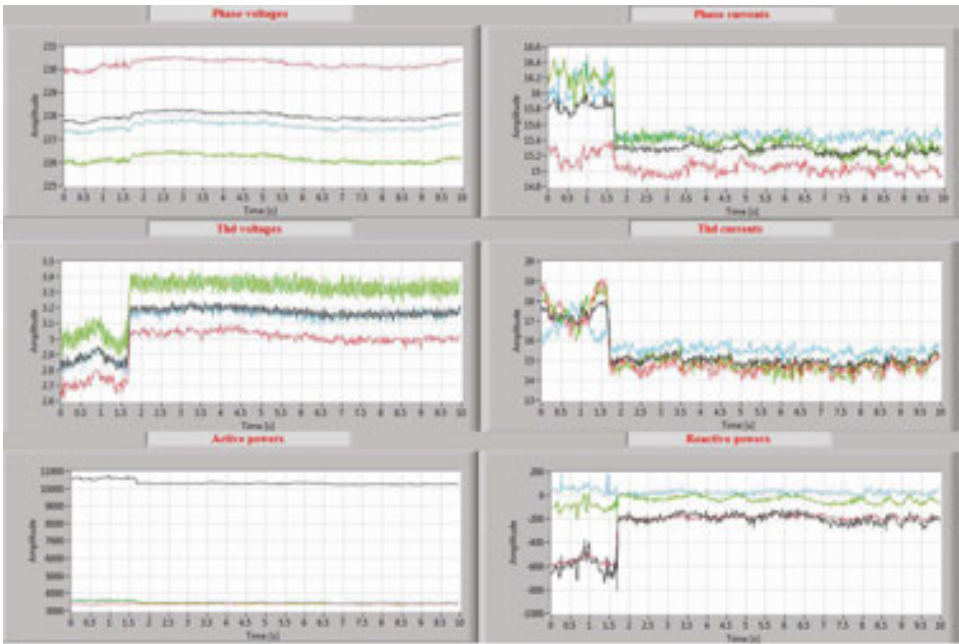


**Figure 15.** Variation of the electrical parameters, passive and active filtering,  $P = 4.5$  kW.



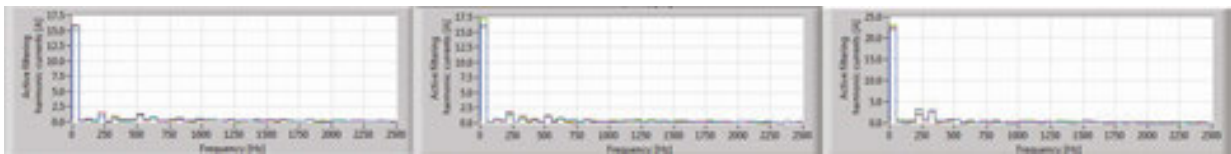


Figure 16. Variation of the harmonic current spectrum with passive and active filtering system.

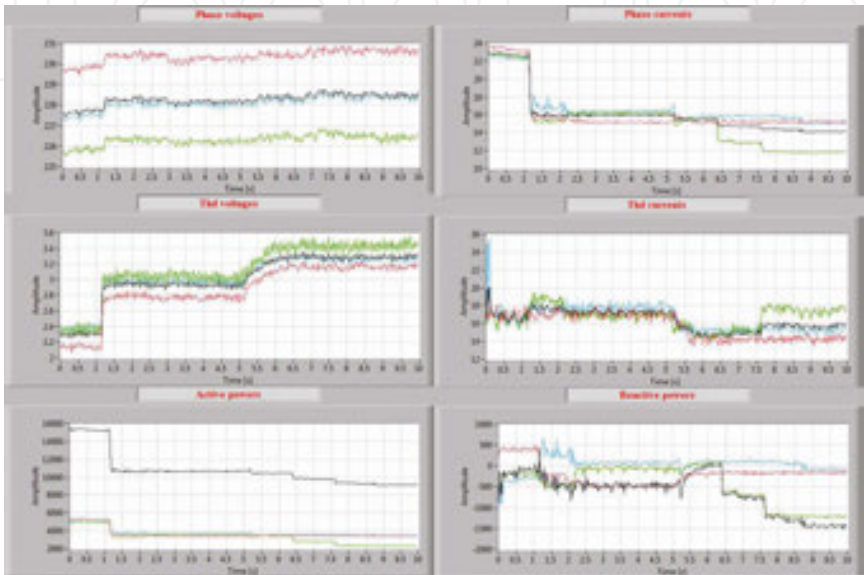


Figure 17. Variation of the electrical parameters, passive and active filtering,  $P = 15$  kW.

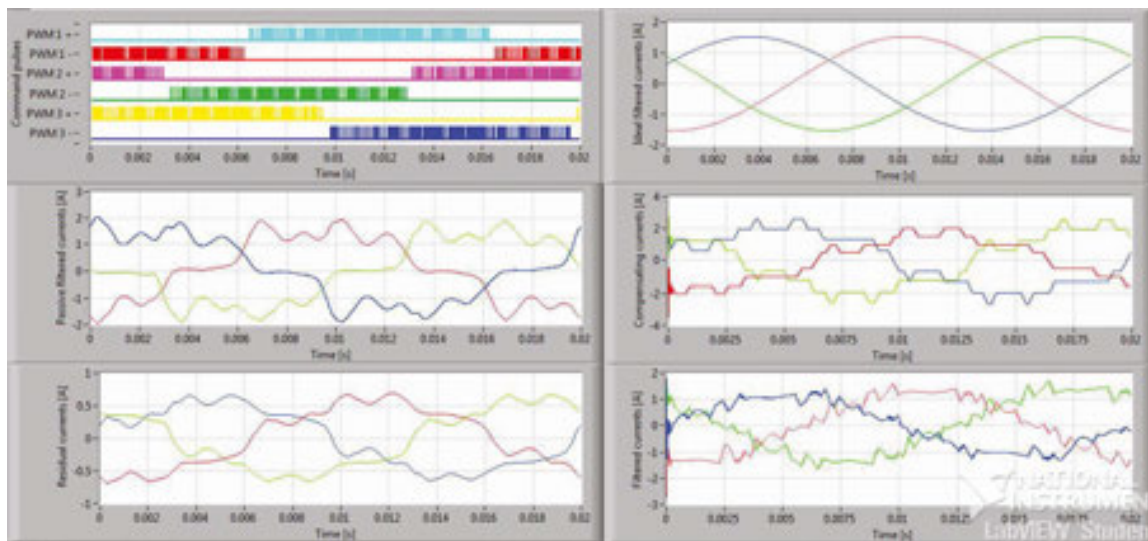
Active power (kW)	Harmonic currents (A)											
	Rank →	1	3	5	7	9	11	13	15	17	19	21
1.5		14	–	2	4	–	3	2	–	–	–	–
3		15	–	2	4	–	2	2	–	–	–	–
4.5		15	–	2	1	–	2	1	–	–	–	–
6		15	–	2	3	–	1	1	–	–	–	–
7.5		15	–	3	2	–	1	1	–	–	–	–
9		16	–	2	1	–	1	1	–	–	–	–
10.5		16	–	2	2	–	1	1	–	–	–	–
12		18	–	3	3	–	1	1	–	–	–	–
13.5		20	–	2	3	–	1	1	–	–	–	–
15		21	–	3	3	–	1	1	–	–	–	–

Table 7. Harmonic currents with passive and active filtering system.



In **Figures 15** and **17**, the variation of the electrical parameters is presented when the passive and active filtering system is connected and **Figure 16**, variation of the current harmonic spectrum, is presented.

The variation on 0.02 s of the active filter signals is presented in **Figures 18–22**, during the functioning of the electrothermal installation at nominal power of 15 kW. The active filtering system generates an input signals soft compensation; therefore, the phase currents get more sinusoidal. This achievement is followed by the total harmonic distortion of the phase currents that is decreased. These parameter variations are obtained by choosing the modulation frequency  $f_m$  of the active filter at the following values: 12,500, 10,000, 5000, 4000 and 2500 Hz.



**Figure 18.** Variation of the active filter signals,  $P = 15$  kW,  $f_m = 12,500$  Hz.

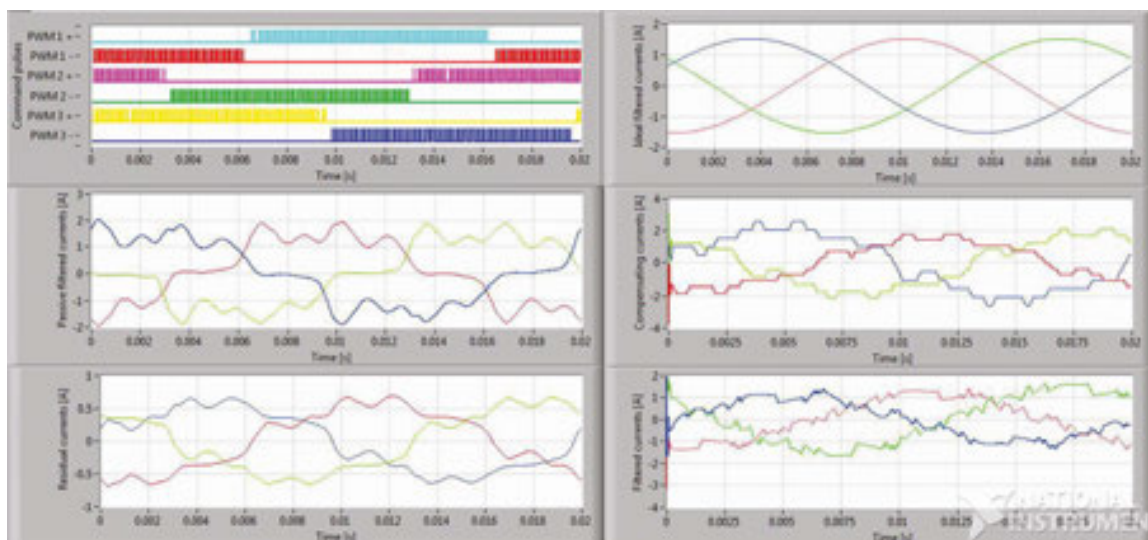


**Figure 19.** Variation of the active filter signals,  $P = 15$  kW,  $f_m = 10,000$  Hz.

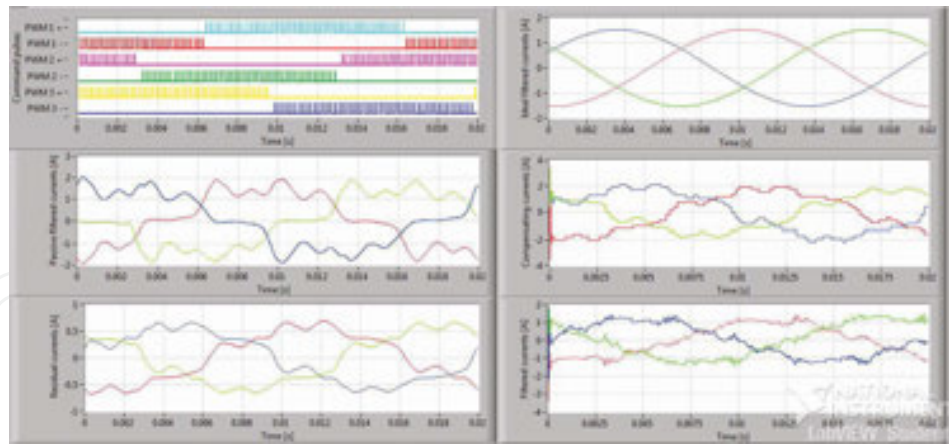


**Figure 20.** Variation of the active filter signals,  $P = 15$  kW,  $f_m = 5000$  Hz.

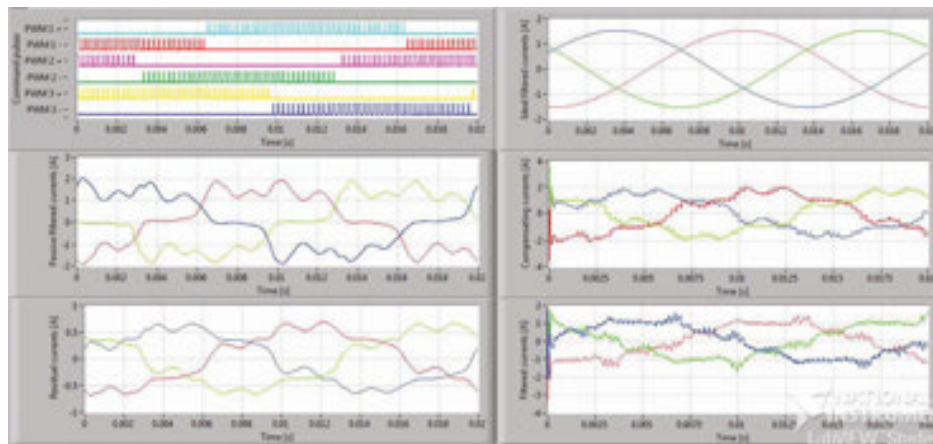


**Figure 21.** Variation of the active filter signals,  $P = 15$  kW,  $f_m = 4000$  Hz.

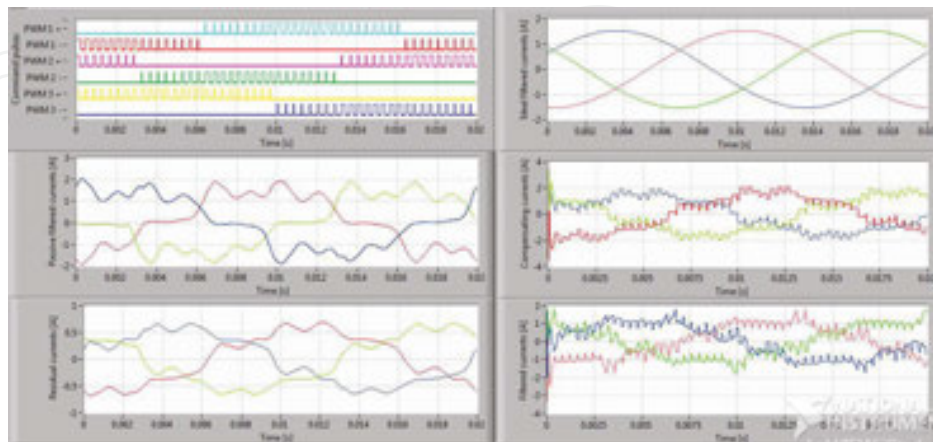


**Figure 22.** Variation of the active filter signals,  $P = 15$  kW,  $f_m = 25,000$  Hz.

By choosing the active filter modulation frequency, the following signals are depicted:

- *Commanding pulses* represent the signals that are generated by PWM modulator subroutine. The commanding signals represent pulses with variable duration and constant amplitude, they being proportional with the distorted signal sample amplitudes, which are assumed into the active filter application. PWM1+ signal represents the PWM modulation of the positive cycles of the phase 1, and PWM1– signal represents the PWM modulation of the negative cycles of the phase 1 and so on.
- *Passive filtered current signals* represent the phase currents, which are assumed using this system when the passive filter system is connected.
- *Residual current signals* represent the current signals that must be compensated.

*Ideal filtered current signals* are ideal-simulated filtered currents.

- *Compensating current signals* are the signals generated by the active filtering system.
- *Filtered current signals* represent the phase currents generated by using the passive and active filtering system.

The colour signification is presented in the following: cyan for PWM1+, red for PWM 1–, magenta for PWM 2+, green for PWM2–, yellow for PWM 3+ and blue for PWM 3–. In the other figures, phase 1 is red, phase 2 is green and phase 3 is blue. The phase currents are represented in red for phase 1, green for phase 2 and blue for phase 3.

In **Table 8**, the variation of THD of the phase currents is synthesized, when the electrothermal installation is equipped with passive filters and also with the entire filtering system, that is, passive and active filtering system.

Active power (kW)	THD (%) Passive filtering	THD (%) Passive + active filtering for $f_m =$				
		12,500 Hz	10,000 Hz	5000 Hz	4000 Hz	2500 Hz
1.5	28	16	1.5	28	16	1.5
3	33	17	3	33	17	3
4.5	39	17	4.5	39	17	4.5
6	37	20	6	37	20	6
7.5	42	20	7.5	42	20	7.5
9	45	19	9	45	19	9
10.5	45	18	10.5	45	18	10.5
12	55	21	12	55	21	12
13.5	60	17	13.5	60	17	13.5

**Table 8.** Variation of THD of the phase currents.

A very important conclusion regarding the electrical parameter variation is the voltage balancing [7]. The phase voltages are constant [8] during the 10% increase of the consumed power of the installation and they are situated between 227.5 and 228.8 V in **Table 4** and also in **Table 6**.

### 3. Conclusions

This paper describes an intelligent system, which is able to command and control an active filtering system using a software application and a data acquisition board.

The electrothermal installation, which is equipped only with passive harmonic compensation devices, generates distorted regime into the power system.

When the active filtering system is connected, the effective values of the phase currents increase from 23 to 28 A. Another important conclusion is the voltage balancing.

The electrothermal installations with electromagnetic induction are current harmonic sources. Therefore, the low values of the total harmonic distortion of the phase voltages and the very high values of the total harmonic distortion of the phase currents are obtained. As it can be seen in **Table 4** and also in **Table 6**, THD for phase voltages lays in standard limits. The most important improvement that is reached in the present study consists in decreasing the phase currents' THD when the active filtering system is connected, from 60 to 17%. This is due to decreasing of the distorted power from 10,000 to 2500 VAd when the active filtering system is connected.

Concerning the variation of the active filter signals, it can be concluded that the number of pulses for each cycle is decreased with the decreasing of the modulation frequency. The duration of the pulses becomes proportionally higher because the pulse-frequency generation by the LabVIEW appropriate functions decreases. The active filter presents the highest accuracy when the modulation frequency is chosen on a maximum level (12,500 Hz), because a less number of samples from the input signals are processed. Therefore, the amplitude of the unwished oscillations, which overlaps the filtered signals, can be neglected. The level of these oscillations is decreasing with the increasing of the modulation frequency.

The monitoring and filtering system presented in this chapter represents an alternative method to the classical harmonic compensation systems, which determines high costs [9]. The software and devices described here represent laboratory equipment, which has great advantage for permanent improvement.

### Acknowledgements

This work was supported by a grant from the Romanian National Authority for Scientific Research and Innovation, CNCS – UEFISCDI, project number PN-II-RU-TE-2014-4-1788.



## Author details

Raluca Rob\*, Gelu Ovidiu Tirian and Caius Panoiu

\*Address all correspondence to: [raluca.rob@fih.upt.ro](mailto:raluca.rob@fih.upt.ro)

Department of Electrical Engineering and Industrial Informatics, Faculty of Engineering  
Hunedoara, Politehnica University of Timisoara, Romania

## References

- [1] F. Hideaki, A. Hirofumi. The unified power quality conditioner: the integration of series and shunt-active filters. *IEEE Transactions in Power Electronics*. 1998;13(2):315–322.
- [2] K. Wada, T. Shimizu. Mitigation method of 3rd-harmonic voltage for a three-phase four-wire distribution system based on a series active filter for the neutral conductor. *IEEE IAS Annual Meeting*. 2002;1:64–69.
- [3] F. Z. Peng, H. Akagi, and A. Nabae. A new approach to harmonic compensation in power systems – a combined system of shunt passive and series active filters. *IEEE Transactions on Industry Applications*. 1990;26(6):983–990.
- [4] P. W. Hammond. A new approach to enhance power quality for medium voltage ac drives. *IEEE Transactions on Industry Applications*. 1997;33(1):202–208.
- [5] W. Tangtheerajaronwong, T. Hatada, K. Wada, and H. Akagi. Design and performance of a transformerless shunt hybrid filter integrated into a three-phase diode rectifier. *IEEE Transactions on Power Electronics*. 2007;22(5):1882–1889.
- [6] Z. Pan, F. Z. Peng. A sinusoidal PWM method with voltage balancing capability for diode-clamped five-level converters. *IEEE Transactions on Industry Applications*. 2009;45(3):1028–1034.
- [7] A. Iagar, G. N. Popa, and C. M. Dinis. The influence of home nonlinear electric equipment operating modes on power quality. *WSEAS Transactions on Systems*. 2014;13:357–367.
- [8] M. Panoiu, F. Neri. Open research issues on modelling, simulation and optimization in electrical systems. *WSEAS Transaction on Systems*. 2014;13:332–334.
- [9] G. N. Popa, S. Deaconu, C. M. Diniş, and A. Iagăr. A case study of an analogical distance relay for the 110kV electric power lines. *WSEAS Transactions on Systems*. 2010;9(10):1063–1072.